
TMD-8
LP
PF-6
WP
PF-3
PF-4
PF-2
LY3
HBL-1
Granta
PF-5
JMP-1
LY10
U2932
HF
DBr
Z-138
PF-1
LR
FN
Toledo
REC-1
DS
TJ
Jeko-1
CJ
DB
OCI-LY19
MZ
MS
LVP-03
McA
Pfeiffer
BJAB
HB
HT
Mino
DB-sp53
RC
SUDHL-10
Maver-1
EJ
DOHH2
JVM-13
SUDHL-4

	PF-2	PF-3	PF-4	PF-5	PF-6
CD5	-	-	-	-	-
CD10	-	-	-	-	-
CD19	+	+	+	+	+
CD20	+	+	+	+	+
CD22	+	+	+	+	+
CD23	+	+	+	+	+
CD43	+	+	+	+	+
CD44	+	+	+	+	+
CD200	+	+	+	+	+
CD3	-	-	-	-	-
CD4	-	-	-	-	-
CD8	-	-	-	-	-
kappa	+	-	+	-	-
lambda	-	+	-	+	+
CD30	+	+	+	+	+
CD11c	-	-	-	-	-
CD56	-	-	-	-	-
CD38	+	+	+	+	+
CD123	+	+	+	+	+
PD-L1	+	+	+	+	+
EBV	+	+	+	+	+

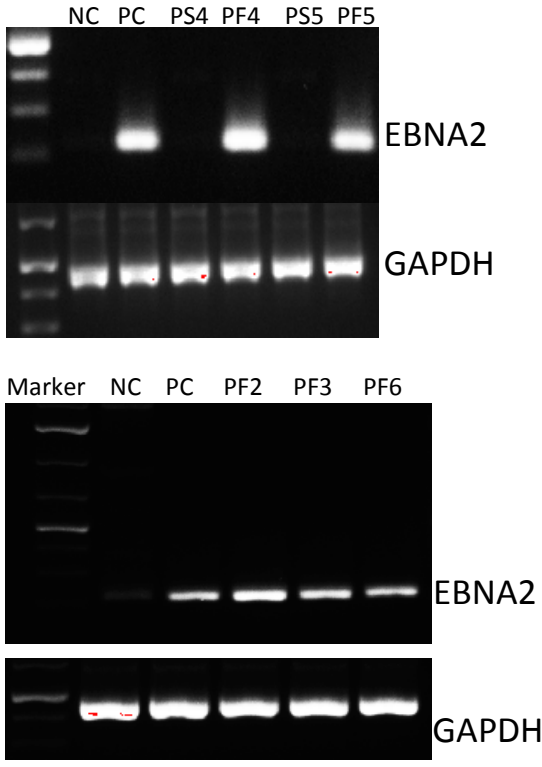

Supplementary Figure 2. Characterization of EBV+ B-cell lymphoma cell lines. PF-2, PF-3, PF-4, PF-5, and PF-6 cell lines were established from apheresis samples obtained from patients diagnosed with mantle cell lymphoma (MCL). Phenotypically, these cells do not express CD5, which is a marker for MCL. They do, however, express both CD19 and CD20, and are considered B cells. Although the patient samples were EBV negative, the established cell lines expressed EBNA2 gene, indicating that these cells acquired EBV during tissue culture. The origin of these cell lines is still unclear, but the expression of CD44, CD123, and CD200 on these cells suggest that they could be derived from stem cells. Most importantly, all these cell lines express PD-L1 protein, indicating that these cell lines represent excellent in vitro models for our current studies. NC, negative control; PC, positive control; PS, patient sample.

Supplementary Figure 2

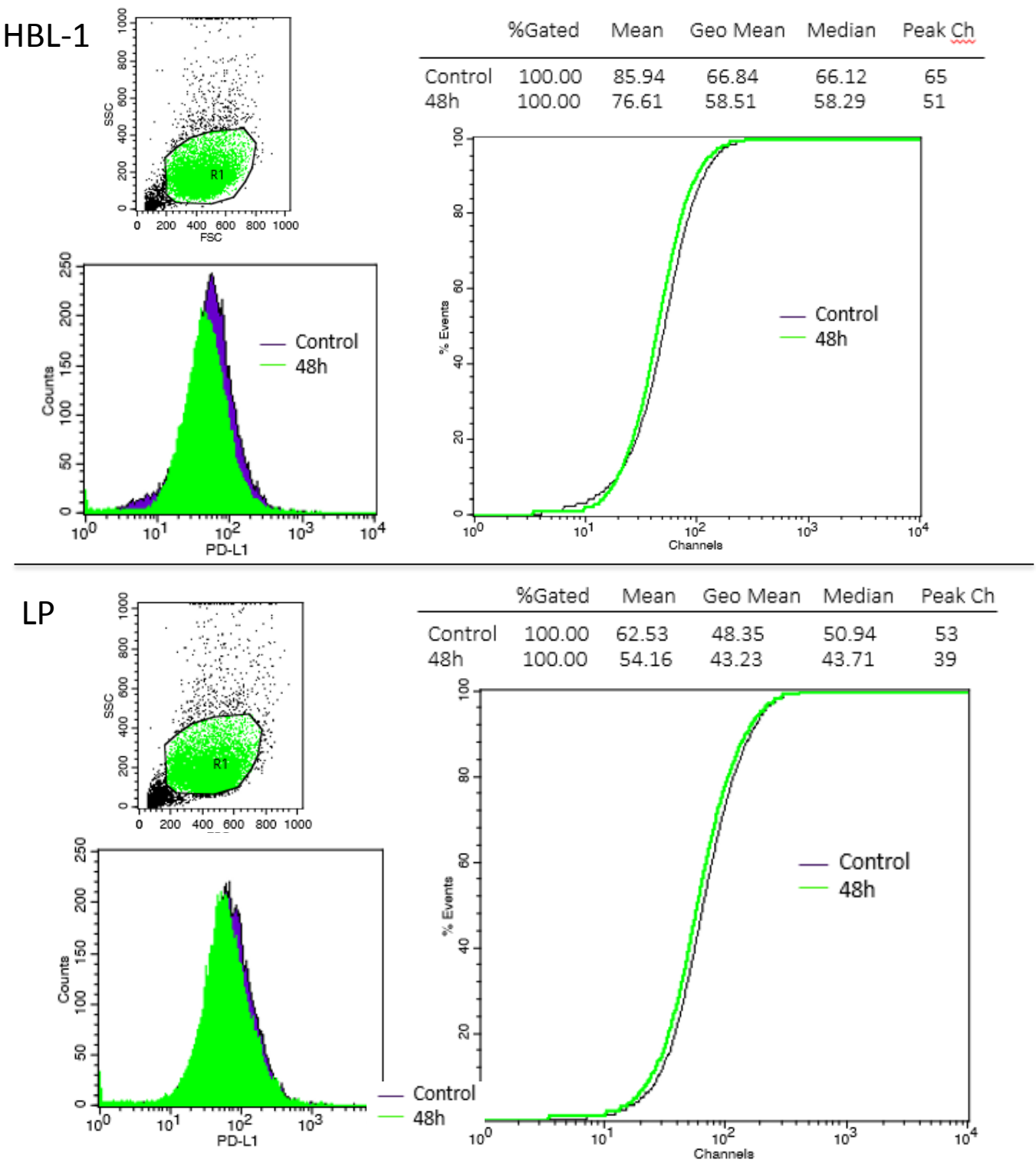

Supplementary Figure 3. Down modulation of membrane PD-L1 expression in DLBCL cells after ibrutinib treatment. Ibrutinib down-regulates PDL-1 molecule expression of Non-GCB cell lines. Non-GCB cell lines HBL-1 and LP were treated with BTK inhibitor, ibrutinib (500nM) for 48h, then analyzed by flow cytometry. Logical gatting were used to identify the expression of PDL-1 on surface of the cell lines. The fluorescence intensity histogram plot of control and 48h ibrutinib treatment samples were over lay to analyze the differences between them. Histogram Statistics and Kolmogorov-Smirnov Statistics were analyzed by CellQuest Pro. The differences between control and treatment group in both cell lines were statistically significant ($p<0.001$).

Supplementary Figure 3

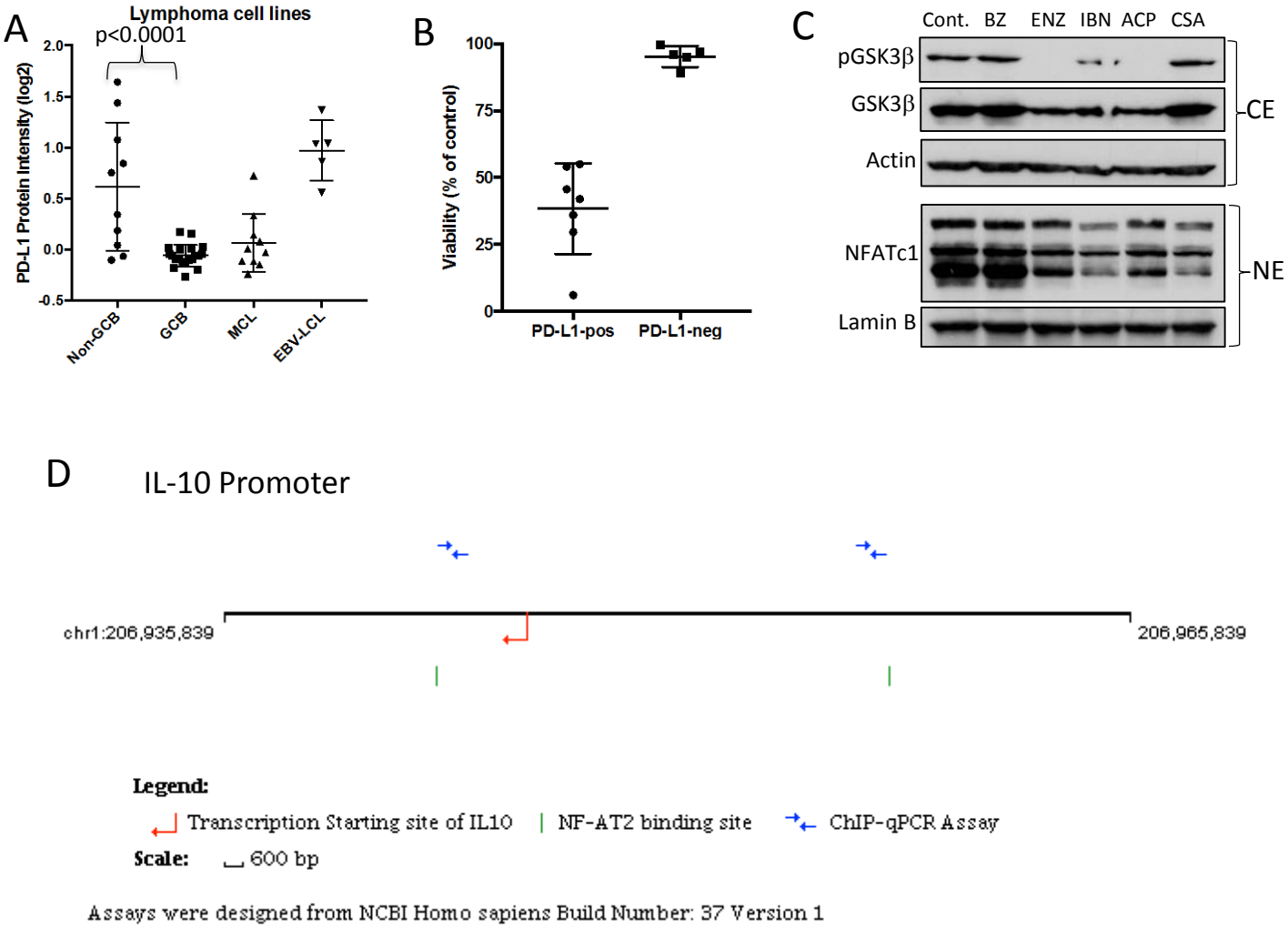

Supplementary Figure 4. Mechanistic mechanisms regulating PD-L1 expression in DLBCL. (A) Scattered plot comparing PD-L1 protein intensity, obtained by RPPA analysis demonstrated in Figure 1A, non-GCB, GCB, MCL, and EBV+ B-cell lymphoma cell lines.. (B) OCI-LY10 cells were treat with a proteasome inhibitor (bortezomib (BZ)), a GSK3β inhibitor (Enzastaurin (ENZ)), BTK inhibitors (Ibrutinib (IBN); ACP-196 (ACP)), or cyclosporine A (CSA) for 24 hours. Purified cytoplasmic extracts were subjected to Western blotting for pGSK3β, GSK3β, and Actin, while nuclear extracts were subjected to Western blotting for NFATc1 and Lamin B. (C) Promoter region of the IL-10 gene. Blue arrows represent potential NFATc1 DNA binding sites.

Supplementary Figure 4

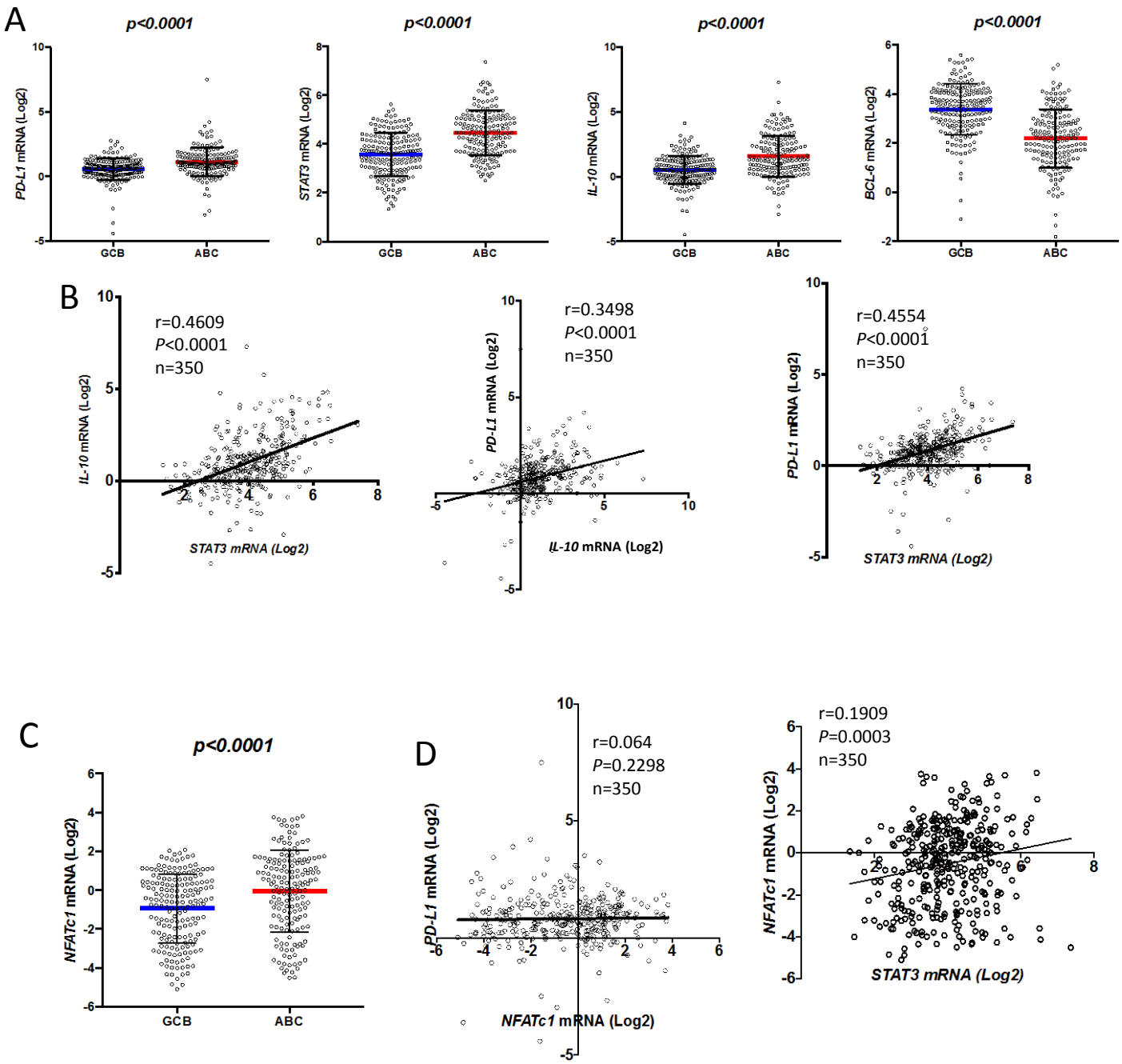

Supplementary Figure 5. Validation of the PD-L1 signature in primary DLBCL samples. Scattered plots comparing *PD-L1, STAT3, IL-10, and BCL-6* mRNA expression levels in GCB vs. ABC-DLBCL subtypes. (B) Spearman's correlation method was utilized to compare the mRNA expression levels of *STAT3, PD-L1*, and *IL-10* genes in primary DLBCL samples (n=350 cases). Data were extracted from Lenz G, et al, from the Oncomine data base. (C) Scattered plots comparing *NFATc1* mRNA expression levels in GCB vs. ABC-DLBCL subtypes. (D) Spearman's correlation method was utilized to compare the mRNA expression levels of *NFATc1 vs. PD-L1 and STAT3* genes in primary DLBCL samples (n=350 cases). Data were extracted from Lenz G, et al, from the Oncomine data base.

Supplementary Figure 5